NEGATIVE SKIN FRICTION INDUCED ON SINGLE PILE IN COLLAPSIBLE SOILS DUE TO TOP INUNDATION

Roy, C.[1], Noor, S.T.[2], Niloy, T.M.[3], Trisha, A.H.[4], Rana, M.[5] and Aziz, T.[6]

[1] *Graduate Student, Department of civil engineering, University of Asia Pacific, Bangladesh, e-mail: chiranjib.uap@gmail.com*
[2] *Associate Professor, Department of civil engineering, University of Asia Pacific, Bangladesh, e-mail: sarah@uap-bd.edu*
[3,4,5,6] *Graduate Student, Department of civil engineering, University of Asia Pacific, Bangladesh, e-mail: tmniloy@gmail.com*

ABSTRACT

The collapsible soil is known as problematic soil, which possesses considerable strength when it is dry and loses its strength and experience excessive settlement when inundated. Moreover, Inundation of any soil is practically unavoidable, as it could take place either naturally or accidentally. Top inundation comes about due to surface runoff, percolation of rain-water, poor drainage, flood etc. Practicing engineers face enormous challenges when they build on/in collapsible soil and as there is lack of sufficient and reliable methods for predicting negative skin friction (NSF) and drag force on piles embedded in collapsible soils, the foundation design in collapsible soil is still based on conventional soil mechanics, which yields unsafe design values. From this paper, however, they will get an insight into the problematic behavior of collapsible soil and associated foundation problems during inundation. This thesis work also attempted to perform a parametric study to establish the effect of the governing parameters that may affect the performance of a single pile in collapsible soil subjected to inundation. In this study, an extensive numerical investigation was carried out using the numerical model to predict NSF exerted on the pile for a given soil and pile conditions due to soil inundation. An analytical model was developed based on the numerical results obtained from the previous investigation to calculate the drag load as well. The results revealed that the value of the average negative shear stress usually varied between 12 to 30 KPa. Whereas, the unit NSF ($Q_n/\pi D$) already reaches its maximum value due to the wetting of 7 m radius front. Beyond this level, the soil becomes detached from the pile. Therefore, any increase in the radius of wetting front and the collapse potential could not further increase the value of NSF.

Keywords: *Collapsible Soil, Top Inundation, Negative Skin Friction, Drag Load and Analytical Modeling.*

1. INTRODUCTION

In recent years, several landslides were experienced suddenly after heavy rainfall in Chittagong hill tracts, Bangladesh, while significant soil settlements near riverside zones have also been reported. Though the causes of both types of disasters have not yet been studied, the consequences resemble inundation induced collapse problem that is commonly observed in arid and semi-arid climatic zones of USA, China, Algeria, Egypt, Russia, etc. Collapsible soils are known to experience significant volume decrease due to the increase of soil moisture content, without an increase in the in-situ stress level. Such soil response (i.e., landslides or significant soil settlements) to inundation could not be predicted beforehand, based on the knowledge of saturated soil mechanics and the experiences with non-problematic or other kinds of problematic (for example, expansive soil and sensitive clay) soils as well. The irrecoverable volume reduction (under constant stress level and only due to the inundation) of collapsible soil takes place so fast and hasty that no measures can be taken to forefend the problem once it initiates.

The problem of negative skin friction (NSF) is the most common problem in the design of pile foundations in soft ground (Lee, Bolton & Al-Tabaa, 2001). In the literature, several reports can be found dealing with negative skin friction on pile foundations, the majority of them dealing with soft soils, while few address the case of collapsible soils, and accordingly, there is a high level of uncertainty for predicting negative skin force on these piles in collapsible soil subjects to top inundation. Negative skin friction mobilizes on piles when the surrounding soil's settlement is faster than the settlement of the pile, resulting in friction force acting downward on the pile shaft (Chen, Huang, Qin & Fang, 2008). The collapsible soil is known as problematic soil that is susceptible to a large and sudden reduction in volume upon wetting. However, inundation of any soil is practically unavoidable, since it could take place either naturally (due to rainfall) or accidentally (e.g., leakage from underground waterlines). Likewise, the most significant, top inundation is brought about due to surface runoff, percolation of rain-water, poor drainage, flood etc. Therefore, piles installed in collapsible soils are subjected to negative skin friction due to the excessive settlement accompanied during inundation from the top. The collapse behavior is governed by some parameters including the collapse potential, the method of inundation and the thickness of the collapsible layer. In this investigation, a prototype experimental model was built to measure negative skin friction forces acting on an end-bearing pile embedded in the collapsible soil during top inundation. The drag load on the pile shaft was also measured as the governing parameters.

Drag load that is induced on the pile as an additional load due to negative skin friction conventionally develops on the pile surface, which needs to be considered in pile design (Noor, Hanna & Mashhour, 2013). If drag load is not considered in the design, it may cause serious damage to structures and might have even lead to catastrophic failure. Piles in the collapsible soil, soft clay, and liquefiable soil may experience drag load due to inundation (Chen, Zhou & Chen, 2009), consolidation (Hanna & Sharif, 2006) and liquefaction (Fellenius & Siegel, 2008), respectively. Lowering of the ground water table around the pile shaft can also cause drag load (Lee, Chen & Wang, 1998). In such cases, pile foundation is often considered the only alternative to transfer loads to the stable soil strata. This is because different soil improvement measures are available, but the extent to which the soil improvement attained in the field condition would adequately minimize the problem of foundation settlement has not been revealed. Previous studies investigated the negative skin friction developed on the pile surface due to inundation of collapsible soil at depth (Hanna and Mashour, 2016; Noor, 2017a and Noor 2017b).

In this study, the effect of inundation of collapsible soil existing near the ground on the development of negative skin friction has been studied. An extensive numerical investigation was carried out to identify the parameters (such as collapse potential, the radius of wetting etc.) and the effects of such parameters on the development of NSF resulting from the full inundation of a given collapsible layer in a single event as well. This paper has also introduced the analytical models, developed by Noor (2011), to predict the drag load on pile due to NSF, caused by the inundation of collapsible soil around the pile. Therefore, by this study, the practicing geotechnical engineers will get an insight about the pile design problems in collapsible soil subject to inundation and thus take part in sustainable development in construction works in our country by addressing these problems.

2. METHODOLOGY

2.1 Numerical Modeling

An axisymmetric finite element model of a single vertical pile was developed to predict negative skin friction for quantifying the drag load. The vertical boundaries were restrained in the horizontal direction, but free to move in the vertical direction. The bottom of the mesh was restrained in both the horizontal and the vertical directions. Therefore, the vertical

settlements of the pile and the soil can occur because of external load and/or the occurrence of inundation of collapsible soil. The centerline of the mesh coincides with the axis of the pile. Both the soil and the pile clusters were meshed with the 15-node triangular element, giving a fourth order interpolation for displacements. Five-node line elements were used at the pile-soil interface to account for the relative pile-soil movement. Figure 1(a) presents the applied boundary condition of the axisymmetric model of a pile embedded in a deep soil bed. The generated mesh, as shown in Figure 1(b), was of medium coarseness using the software *PLAXIS, 2D*.

Important mesh parameters, including size and types of elements and mesh coarseness, were provided to generate mesh automatically, skipping a laborious job of defining thousands of nodes and elements manually. Some important issues were given special attention in generating mesh. First of all, very coarse and very fine meshes were not created to avoid large errors in results and to reduce excessive computational time, respectively. Based on the experience, global fine mesh was considered inappropriate for the problem in hand, as it also involves excessive number of total DOFs. On the other hand, an acceptable mesh demands relatively large number of nodes in the vicinity of the pile's shaft, as deformations and stresses generally vary significantly around the pile and at the interface, respectively, as the objective of this modeling is to investigate shear stress distribution at the pile-soil interface.

Mesh is considered acceptable, if it does not include any elongated element and aspect ratio ranges within the reasonable range. However, medium global coarseness applied all over cannot dispense the accuracy in results up to the mark. Therefore, considering the mesh dependency of the FEM results, mesh refinement technique was adopted in this study. A zone, 3 m horizontally from the pile axis and 1.5 L from the ground, was considered for this local mesh refinement. Secondly, any quick transition of element size (between the global elements and those in the refined mesh zone near the outer boundary of the refined mesh zone) was eliminated as the initial mesh was generated with medium global coarseness. Thirdly, the graphical display of the generated mesh was visually inspected for any possible errors, related to the shape of elements and the aspect ratio. If any element is distorted and/or elongated, the shape of the element is adjusted by refining adjacent geometry lines.
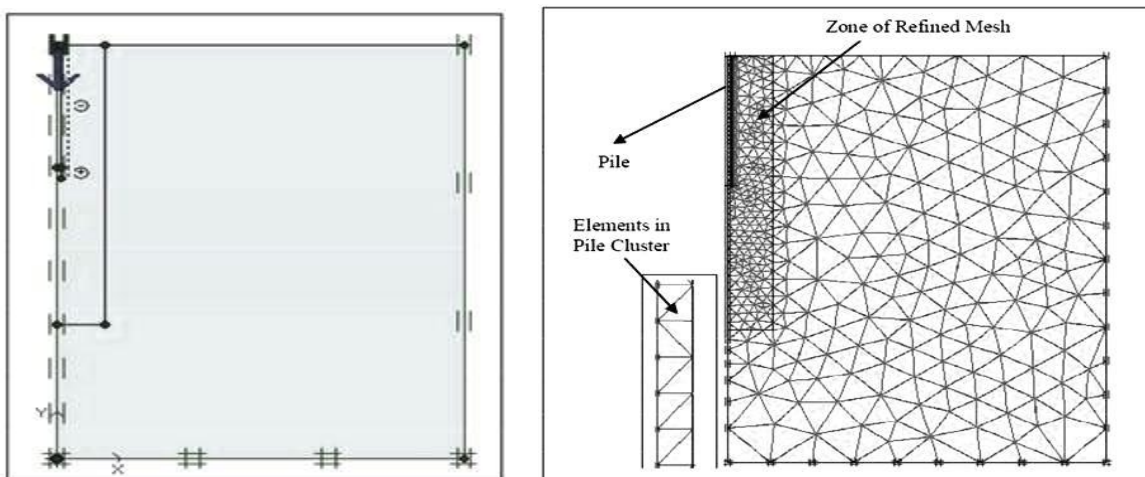

Figure 1: (a) Boundary condition & (b) Generated Mesh in an axisymmetric model.

Pile material was modeled as a non-porous material with Linear-Elastic (isotropic) constitutive relationship, requiring only two input parameters: Young's modulus (E_p) and Poisson's ratio (u_p). The constitutive law of the soil was defined by Mohr-Coulomb (MC) failure criterion, requiring five material parameters; including cohesion (c), the angle of

internal friction (φ), the angle of dilatancy (ψ), modulus of elasticity (E) and Poisson's ratio (υ). The behavior of the pile-soil interface was also defined by the MC Model.

In simulating the inundation of collapsible soil, the procedure given in (Noor et al., 2013) proposed to carry out the finite element calculation in three steps [Steps 1, 2*a* and 2*b*]. Step 1 was for the installation of the pile, step 2*a* was to incorporate the effect of strength reductions due to inundation, and Step 2*b* was to simulate volume reduction of collapsible soil subjected to inundation. While detailing out Step 2*a*, that study addressed only the soils that underwent significant reductions in the initial shear strength parameters.

As the present study simulates the scenario of inundation taking place within the collapsible soil layer (in contact with the pile shaft), the changes in the aspects of collapsible soil due to inundation are considered in developing the numerical model. It is to note that the values of c and φ (*i.e.,* two input parameters) decrease, as matric suction decreases during inundation. Moreover, the friction angle (δ) between the pile and the soil that is the main factor to control the magnitude of pile skin friction also decreases during inundation. In the simulation of the present study, these two aspects were addressed in two steps [Step *2a-1* and Step *2a-2*], as shown in Figure 2. Step *2a-1* is to address the strength reduction of unsaturated soils due to inundation. It was previously noted that reduction in φ value of the soil adjacent to the pile shaft has a minor influence on the magnitude of drag load, as calculated from the *PLAXIS* output. Therefore, Step *2a*-2 is necessary to incorporate the required adjustment of the input parameters' values for pile interface elements to address the changes in the value of the friction angle (δ).

The above numerical model was employed to derive the mathematical functions that define the coefficients of analytical models developed in this study. Hence, the case of a single-vertical pile was modelled for different pile dimensions, soil properties, and inundation conditions, as listed in Table (1). However, in order to develop charts, the study has choosen the ranges of different parameters by giving considerations to the properties of collapsible soil identified by previous researchers.

Table 1: List of Variable Parameters of Collapsible Soil Properties.

Parameters	Unit	Range
Cohesion (c) of collapsible soil	kPa	20
Angle of internal friction (φ_{cs}) of collapsible soil	°	20–40
Collapse potential (C_p)	%	5–15
Angle of internal friction (φ) of dense sand	°	40
Thickness of collapsible soil layer (H)	m	8–15
Depth of collapsing soil (H_s)	m	4–7.5
x = H_s/H	-	0.5
Length of pile (L)	m	12–30
Diameter of pile (D)	m	0.2–1
Pile length-to-diameter ratio (L/D)	-	20–75
Embedded pile length into noncollapsible soil-to-full pile length ratio (L_e/L)	-	0.3–0.75
Radius of wetting (h)	m	3–10
Interface strength reduction factor (ISRF)	-	0.6–0.9

(Noor, 2017)

2.2 Validation of Numerical Model

Firstly, the performance of the developed model and the generated mesh has been tested in terms of ultimate pile capacity, shaft resistance and base resistance of a single pile in dense, medium dense and loose sands using finite element analysis, and the numerically obtained results compare well with those predicted from empirical formulae. Secondly, the validation of the numerical model has been verified by simulating the pile load test in Volgodon experimental region -2 in constant moisture condition. The soil properties of test site have been given in Table (2). The results obtained from numerical analysis have also been found in good agreement (Table 3). Thirdly, the performance of the model in predicting drag load due to negative skin friction due to inundation from the top, was found efficacious with respect to the results of full-scale pile load test in Nikopol region from Grigoryan (1997). Table 4 presents the soil properties used for validation of the numerical model. The comparisons between numerical and experimental results have been given in Table 3. The length-to-diameter ratio (L/D) was 18 and 44 for the piles at Volgodon-2 and at Nikopol, respectively. The collapse potential of the soil up to 6 m below the ground level was 7 %.

Table 2: Soil Properties (Volgodon-2)

Depth (m)	w_n (%)	γ_{bulk} (kN/m^3)	G_s	e	S %	c (kPa)	υ (^{o})	Remarks
0 – 6	13.8	16.95	2.68	0.78	51	15	19	Collapsible
6 – 15	15	17.5	2.69	0.73	56	24	17	Collapsible
15 - 25	17.9	18.82	2.69	0.62	73	33	19	Non-Collapsible, unsaturated
25-35	23.0	19.6	2.69	0.62	100	33	19	Non-Collapsible, saturated

Table 3: Comparison of Results: Collapsible Soil without inundation condition.

Pile Resistances	Present study	Experimental (Grigoryan, 1997)
Ultimate Pile Capacity, Q_u (kN)	3204	3240
Shaft Resistance, Q_s (kN)	2930	2948
End Resistance, Q_b (kN)	274	292

Table 4: Soil Properties (Nikopol)

Depth (m)	w_n (%)	Void Ratio $e_{initial}$	w_{sat} (%)	γ_{sat} (kN/m^3)	c (kPa)	υ ($^\circ$)
0 – 8	7	0.91	28.7	17.57	5	20
8 – 23	4.3	0.86	30.82	18.34	6	16
23 - 30	11.3	0.71	21.2	18.4	5	18

The pile, tested in Nikopol, was equipped with three strain gauge dynamometers at 9.2 m, 12.3 m and 22 m (pile tip) from the pile head. The strain gauge dynamometer was specially

designed with electrical sensors, developed at the Central Scientific Research Institute (TsNIIK in Russian). The dynamometer was installed within the pile stem, so that the full longitudinal force could pass through it. The principle component of a strain gauge dynamometer was the elastic ring, made of high strength steel. The elastic ring was placed between two steel plates of 10 mm thick. The steel plates, with the elastic ring inside, were covered by rubber casings, of 3—4 mm thick. The rubber casing was used for the protection of the steel plates and the elastic ring. Individual pile section was welded to the steel plates. Each cable (wire) attached to the elastic ring was brought to the ground through separate pipe. Pipes were covered with bitumen to prevent cohesion 96 between the pipe and the concrete. In the laboratory, the gauge reading showed no effect of moisture and temperature variations, insulation condition of conductors and oxidation of contacts. Dynamometer measures deformation gave the magnitude of the axial load at the point where it was installed. This dynamometer was calibrated in the laboratory and recalibrated after the pile installed in the ground. The calibration was made up to a load of 1000 kN. The pile was acting under 600 kN load applied at the pile head. The drag load acting on the pile in Nikopol region was 180 kN as measured during field test. The drag load of 186 kN was estimated by numerical analysis of the test pile at Nikopol.

2.3 Analytical Modeling

In this study, the analytical models (developed by Noor, 2011) were employed to predict the drag load (Q_n) due to negative skin friction resulting from the inundation of collapsible soil from the top. Based on the numerical results, unit negative skin friction ($Q_n/\pi D$) has a linear relationship with Hs/D, as defined by Equation (1).

$$Q_n/\pi D = I_a * (H_s/D) + I_b \tag{1}$$

The values of I_a and I_b depend on the collapse potential (C_p), as $Q_n/\pi D$ shows different slopes for different collapse potential (varies between 5–15%) for a given H_s/D ratio. The values of I_a and I_b depend on H_s/D ratio, as shown in Figure 2 and Figure 3.
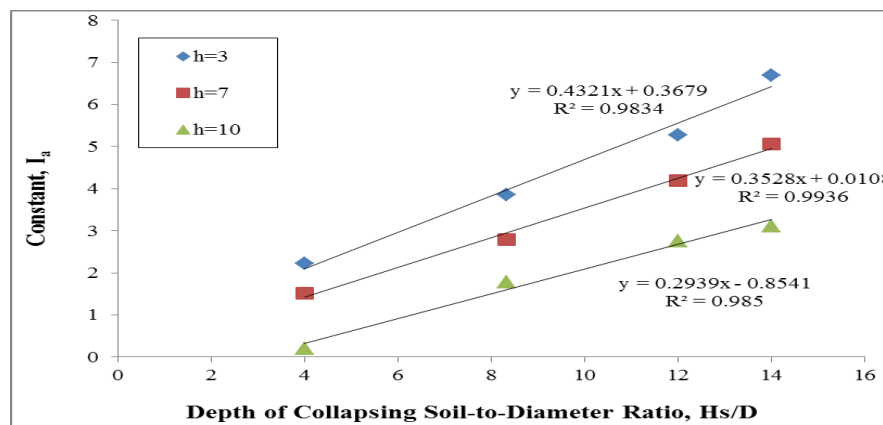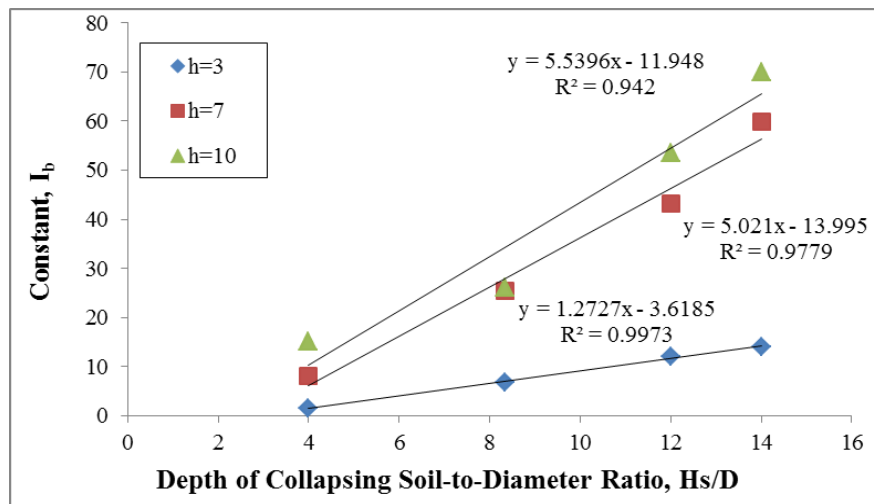

Figure 2: Value of Ia for different Hs/D and h, when Cp between 5–15%.

The value of I_a can be found from Equation (2) – Equation (4) as below.

For h = 3 m
$$I_a = 0.432 (H_s/D) + 0.368 \tag{2}$$

For h = 7 m
$$I_a = 0.353 (H_s/D) + 0.011 \tag{3}$$

For h = 10 m
$$I_a = 0.294 (H_s/D) + 0.854 \tag{4}$$

Figure 3: Value of Ib for different Hs/D and h, when Cp between 5–15%.

The value of I_b can be found from Equation (5) – Equation (7) as below.

For h = 3 m

Ib = 1.273 (Hs/D) – 3.619 (5)

For h = 7 m

Ib = 5.021 (Hs/D) – 13.995 (6)

For h = 10 m

Ib = 5.539 (Hs/D) – 11.948 (7)

Therefore, the indirect load is also known as drag load (Q_n) due to NSF (at ISRF 0.8) can be predicted from the value of the unit negative skin friction using Equation (1) multiplied by the perimeter (πD) of the pile for the case of inundation from the top.

3. RESULTS AND DISCUSSION

The shear stress distribution at the pile interface for a given collapsible soil layer (h=3m) of different collapse potential (Cp) has been illustrated in Figure 4. It is observed that during soil collapse, both the negative shear stress (due to NSF) and the positive shear stress (due to positive skin friction) take place simultaneously. A significant influence of collapse strain (i.e. volume reduction) was also observed due to inundation, such as for greater collapse strain, Q_n increases, because of the increase in the area bounded by the negative part of the shear stress distribution.
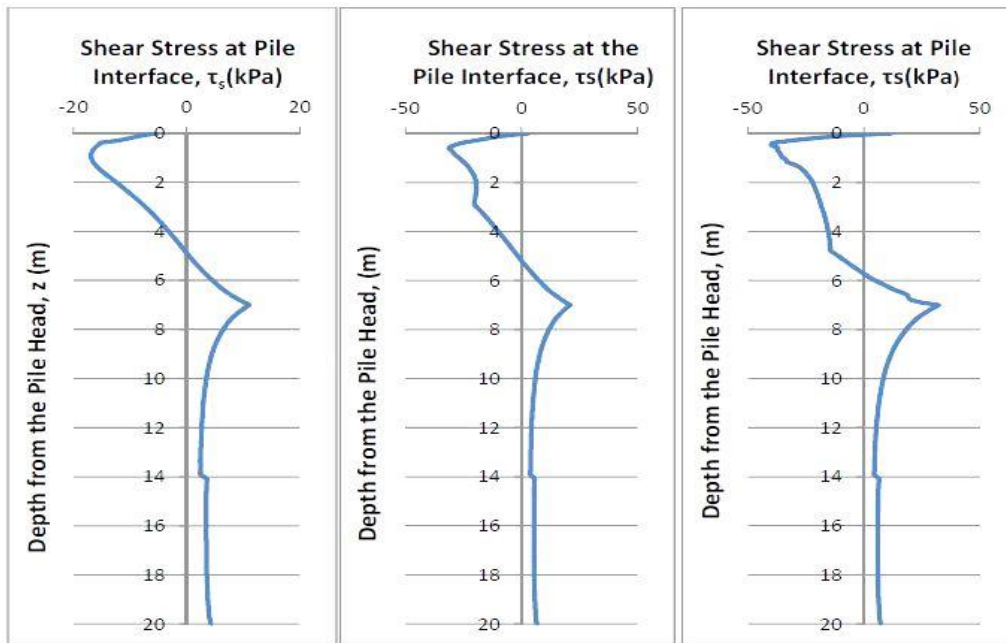
Figure 4: Shear stress distribution, when h = 3m, (a) Cp = 5%, (b) Cp = 10% and (c) Cp = 15%.

The effects of the radius of wetting front (h) on the shear stress distribution were also examined in Figure 5 for the cases of inundation from top. It was investigated that the area bounded by the negative part of the shear stress distribution increases with the increase of the radius of wetting front, and hence, the indirect load (Q_n) due to NSF also increases, accordingly.
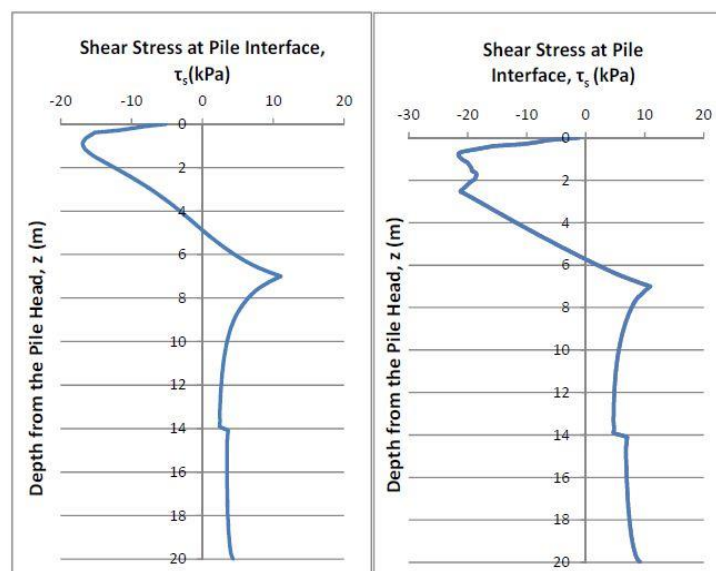

Figure 5: Shear stress distribution, when C_p = 5%; (a) h = 3m, and (b) h =7m.

The effect of the depth of collapsing soil-to-pile diameter ratio (Hs/D) on negative skin friction has been depicted in Figure 6- Figure 8 by turns for different depth of collapsible soil layer, where the unit negative skin friction ($Q_n/\pi D$) shows linear variation with the increase of H_s/D ratio. High collapse potential of the collapsing soil and wide wetting front were also found to increase the intensity of the effect of Hs/D ratio on $Q_n/\pi D$.
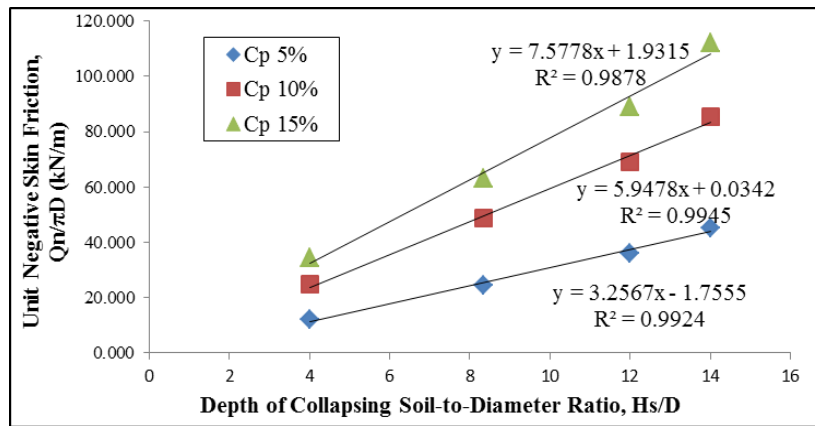
Figure 6: Unit negative skin friction (Qn/πD) vs. Hs/D ratio, when h = 3m.
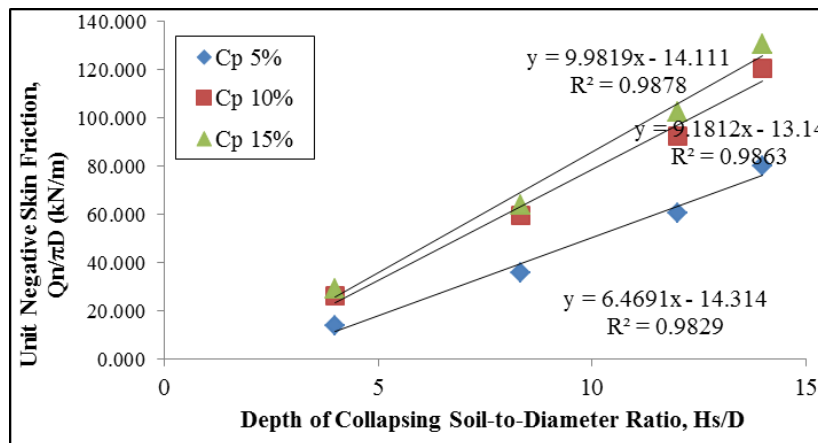
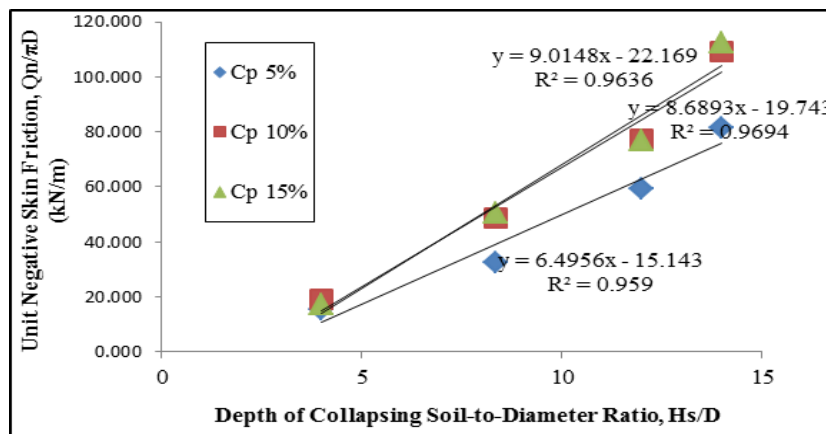Figure 7: Unit negative skin friction (Qn/πD) vs. Hs/D ratio, when h = 7m.

Figure 8: Unit negative skin friction (Qn/πD) vs. Hs/D ratio, when h = 10m.

The effect of the radius of wetting front on Qn/πD for different Hs/D ratio and Cp has been shown in Figure 9- Figure 11 as below. It is found that Qn/πD does not increase infinitely with the increase of h. Figure 11 has demonstrated that Q_n/πD attains its maximum value due to 7 m of the radius of wetting front. Beyond this level, the soil becomes detached from the pile. Therefore, any increase in the radius of wetting front and the collapse potential could not further increase the value of Q_n/πD.
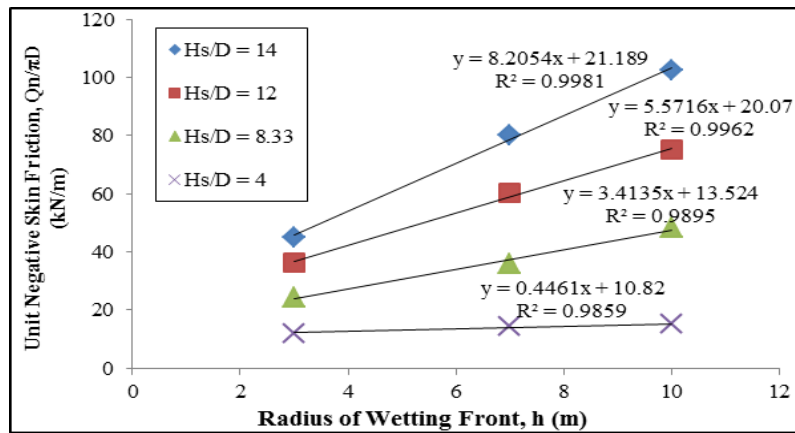
Figure 9: Effect of radius of wetting front (h) on $(Q_n/\pi D)$, when $C_p = 5\%$.
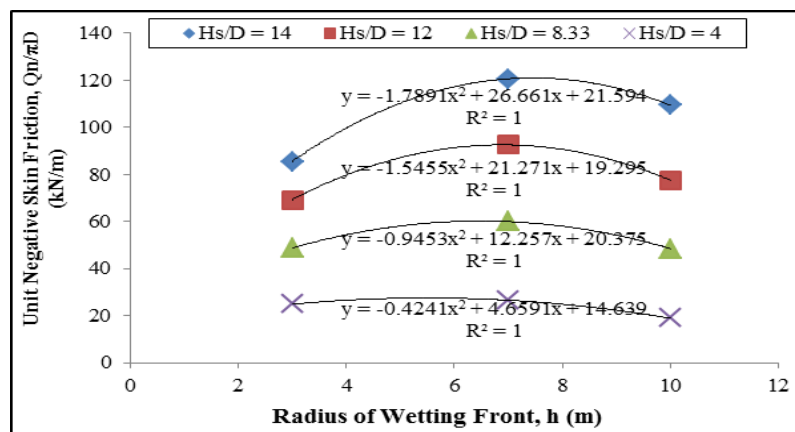
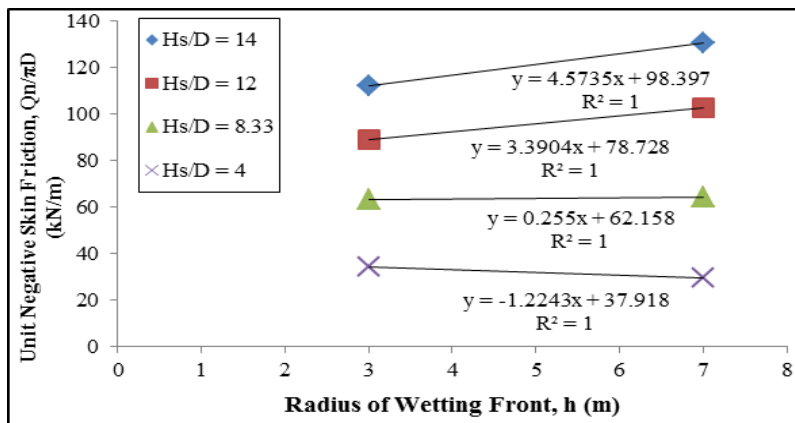Figure 10: Effect of radius of wetting front (h) on $(Q_n/\pi D)$, when $C_p = 10\%$.

Figure 11: Effect of radius of wetting front (h) on $(Q_n/\pi D)$, when $C_p = 15\%$.

The effect of collapse potential (C_p) on $Q_n/\pi D$, for different Hs/D ratio and h, has been demonstrated in Figure 12 - Figure 14. It is noted that there exists a linear relation between average negative shear stress (q_n) and collapse potential (C_p) in each case. For a given radius of wetting front (h), the straight line in q_n vs C_p plot passes through origin. The investigated result reveals that between 5–10% of collapse potential, the effect of C_p is more pronounced than any other condition beyond this range. It can also be noted that the proportional coefficient relating q_n and C_p varies with H_s/D. The value of proportional coefficient also increases if the H_s/D ratio is less than 14, for a given radius of wetting.
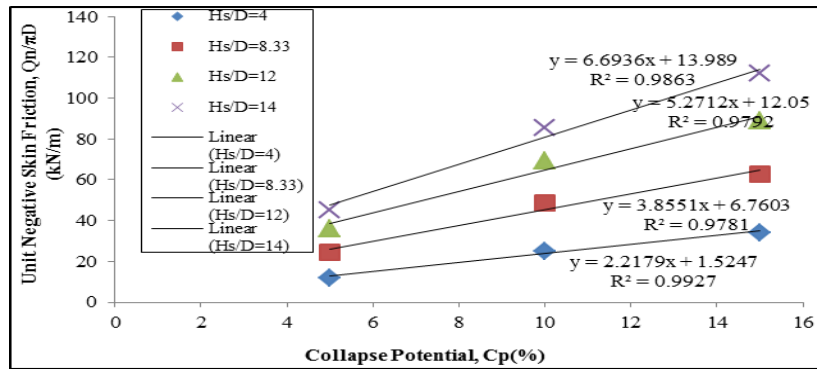
Figure 12: Effect of collapse potential (C_p) on ($Q_n/\pi D$), when h = 3 m.
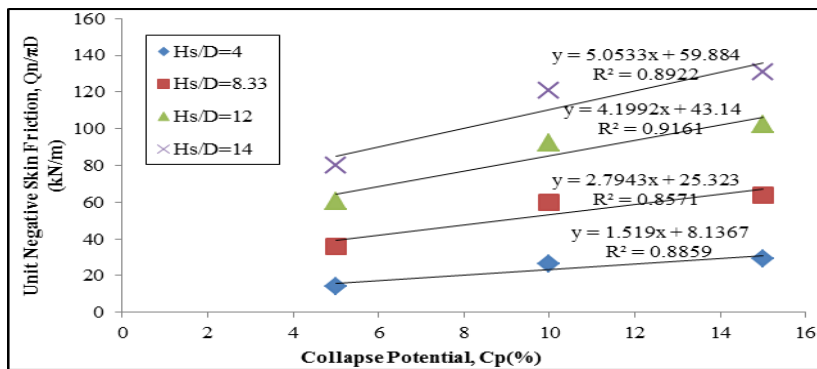

Figure 13: Effect of collapse potential (C_p) on ($Q_n/\pi D$), when h = 7 m.
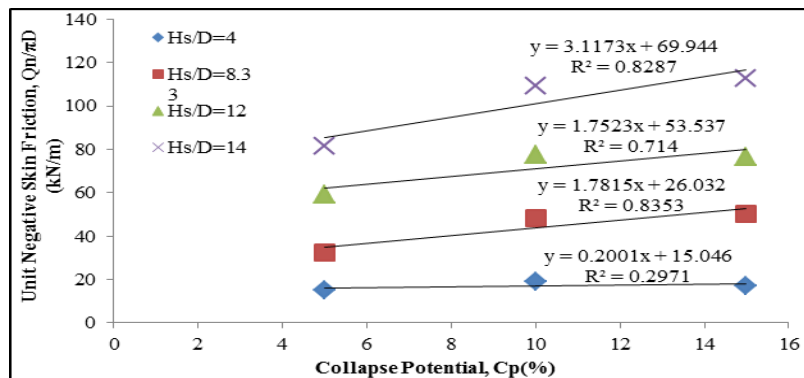

Figure 14: Effect of collapse potential (C_p) on ($Q_n/\pi D$), when h = 10 m.

However, based on the numerical results, collapse potential (C_p), radius of wetting (h), direction of wetting (from bottom or top) and interface strength reduction factor were found to have significant influence on the shear stress developed on the pile interface during inundation of collapsible soil around the pile. Instead, the angle of soil internal friction (φ), L_e/L and L/D ratios have no effect on average negative shear stress (q_n). Furthermore, H_s/D ratio governs the magnitude of average negative shear stress.

4. CONCLUSIONS

The magnitude of the drag load caused by inundation-induced soil collapse adjacent to the pile shaft depends on several parameters, while most of these parameters are not related to the development of drag load due to consolidation or liquefaction. In this study, numerical model is developed considering all the parameters influencing the magnitude of drag load

and the fact that negative skin friction is a kinetic type of friction. The analytical models are developed to quantify the drag load at the design stage. Moreover, the following conclusions could also be summarized based on the scope of this study:

- Unit negative skin friction ($Q_n/\pi D$) has linear relation with H_s/D ratio in a semi logarithmic plot, for given h and C_p.

- Unit negative skin friction ($Q_n/\pi D$) does not increase infinitely due to the increase of h.

- Collapse potential (C_p) influences unit negative skin friction ($Q_n/\pi D$) more than the depth of neutral axis (N.A.).

- The design guideline, presented in this paper, will allow the foundation designers to optimize the pile design diameter.

ACKNOWLEDGEMENTS

REFERENCES

Chen, Z. H., Huang, X. F., Qin, B., Fang, X.W. & Guo, J. F., (2008). Negative skin friction for cast-in-place piles in thick collapsible loess. In: D.G. Toll, C.E. Augrade, D. Gallipoli, and S.J. Wheeler, Eds., *Unsaturated Soils. Advances in Geo-Engineering.,* Taylor and Francis: London, UK, pp. 979-985.

Chen, R.P., Zhou, W.H., & Chen, Y.M., (2009). Influences of soil consolidation and pile load on the development of negative skin friction of a pile. *Comput. Geotech.,* vol. 36, pp. 1265-1271. Retrieved from http://dx.doi.org/10.1016/j.compgeo.2009.05.011.

Fellenius, B.H. & Siegel, T.C. (2008). Pile drag load and downdrag in a liquefaction event. *J. Geotech. Geoenviron. Eng.,* vol. 134, pp. 1412-1416. Retrieved from http://dx.doi.org/10.1061/(ASCE)1090-0241(2008)134:9(1412).

Grigorian, A.A., (1997). *Pile foundations for buildings and structures in collapsible soil.,* A.A. Balkema Publishers: Brookfield, VT.

Hanna, A.M. and Sharif, A., (2006), "Drag force on a single pile in clay subjected to surcharge loading", *Int. J. Geomech.,* vol. 6, pp. 89-96. Retrieved from http://dx.doi.org/10.1061/(ASCE)1532-3641(2006)6:2(89).

Lee, C.J., Bolton, M.D., & Al-Tabaa, A. (2001, April). Recent findings on negative skin friction in piles and pile groups in consolidating ground. Proceedings of the 5th International Conference on Deep Foundation Practice. Singapore. pp. 273-280.

Lee, C.J., Chen, H.T. & Wang, W.H., (1998). Negative skin friction on a pile due to excessive ground water withdrawal. Proceedings of the International Conference. Centrifuge, New York. pp. 513-518.

Noor, S.T., Hanna, A.M., & Mashhour, I., (2013). Numerical modeling of piles in collapsible soil subjected to inundation. *Internatioal Journal on Geomech.,* vol. 13, pp. 514-526. Retrieved from http://dx.doi.org/10.1061/(ASCE)GM.1943-5622.0000235.

Noor, S.T., (2017). Numerical and Analytical Modeling for Predicting Drag Load Induced on Pile in Collapsible Soil because of Inundation. *The Open Civil Engineering Journal*, August, 2017, *11,* pp.664-675. DOI: 10.2174/1874149501711010664. Retrieved from www.benthamopen.com/TOCIEJ/.

PLAXIS 2D 8.6 [Computer Software]. Delft, Netherlands, PLAXIS.